Available online at www.sciencedirect.com
SciVerse ScienceDirect
Procedia CIRP 8 (2013) 265 – 270
www.elsevier.com/locate/procedia

14th CIRP Conference on Modeling of Machining Operations (CIRP CMMO)

Modeling and Simulation of the Electrochemical Machining (ECM) Material Removal Process for the Manufacture of Aero Engine Components

F. Klocke[a], M. Zeis[a,]*, S. Harst[a], A. Klink[a], D. Veselovac[a], M. Baumgärtner[b]

[a]Laboratory forMachine Tools and Production Engineering, Steinbachstraße 19, Aachen 52074, Germany
[b]Leistritz Turbomaschinen Technik GmbH, Markgrafenstrasse 29-39, Nuremberg 90459, Germany
* Corresponding author. Tel.: +49-241-80-27467; fax: +49-241-80-22293; E-mail address: m.zeis@wzl.rwth-aachen.de.

Abstract

In order to increase the efficiency of jet engines hard to machine nickel-based and titanium-based alloys are in common use for aero engine components such as blades and blisks (blade integrated disks). Here Electrochemical Machining (ECM) is a promising alternative to milling operations. Due to lack of appropriate process modeling capabilities beforehand still knowledge based and a cost intensive cathode design process is passed through.
Therefore this paper presents a multi-physical approach for modeling the ECM material removal process by coupling all relevant conservation equations. The resulting simulation model is validated by the example of a compressor blade. Finally a new approach for an inverted cathode design process is introduced and discussed.

Selection and peer-review under responsibility of The International Scientific Committee of the "14th CIRP Conference on Modeling of Machining Operations" in the person of the Conference Chair Prof. Luca Settineri

Keywords: Electrochemical Machining (ECM); simulation; aero engine components; inverse problem

1. Introduction

To achieve weight reduction and increased thermal efficiency of jet engines, hard to machine alloys such as Ti-6Al-4V and Inconel 718 are in common use for the manufacture of aero engine components. Especially the milling process of blisks made of Ni-based alloys reaches its technological and economical limit. Here Electrochemical Machining (ECM) is a cost-effective alternative. In ECM high material removal rates can be realized without developing any white layer or heat affected zone. Additionally via ECM it is possible to achieve finished surfaces qualities during rough machining operations, which eliminates the need for further treatment like cost-intensive finish milling steps or polishing operations [1, 2, 3].

But due to cost intensive tool developing processes and rather high investment costs for the machine tools, ECM is mostly used in productions with large batch sizes. Main reason for high tool costs is an only knowledge-based, iterative cathode designing process. After a test run the produced workpiece has to be measured and the difference between target and actual geometry due to locally changed conditions of electrolysis is subtracted from the cathode and so forth.

On the other hand the theoretic background of the electrochemical material removal process with all its different physical aspects is very well known, but up to now it has never been succeeded to combine all different aspects together into one sufficiently precise model to simulate the process for the manufacture of aero engine components.

This paper presents a new approach for modeling the ECM material removal process by coupling the conservation equations for fluid flow, electric fields, electrochemical surface reactions, ionic transport and heat transfer. Based on initially introduced governing equations, possible coupling strategies are presented and discussed. Afterwards, the aerodynamic cross-section of a compressor blade is calculated in two different ways.

Selection and peer-review under responsibility of The International Scientific Committee of the "14th CIRP Conference on Modeling of Machining Operations" in the person of the Conference Chair Prof. Luca Settineri
doi:10.1016/j.procir.2013.06.100

Besides the simulation of the classical ECM process with the aim to calculate the blade contour by using predetermined cathode geometries a new inverted simulation strategy is presented. This new approach uses the blade target geometry in order to calculate cathode shape by inverting the electric field.

2. Theoretical Backround

ECM is a manufacturing technology where many different physical disciplines and aspects need to be considered (cp. figure 1). In order to simulate this material removal technology besides the modeling of the electromagnetic field the electrolyte flow has to be calculated, as well as the reactions on electrode's surface and the ionic transport.

So in this chapter the governing equations for a complete description of the electrochemical material removal process are named and possible physical couplings are discussed.

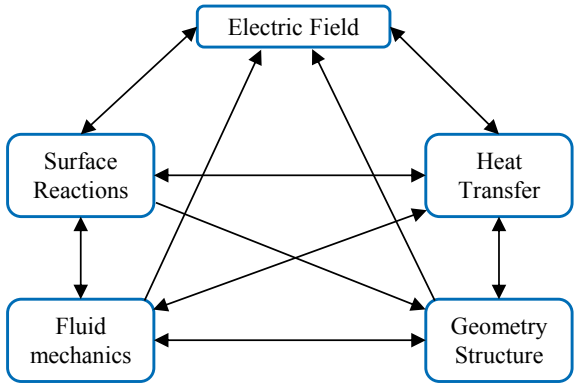

Fig. 1. Physical Couplings in ECM [4]

2.1. Electric Field

The electric field forms the basis for electrochemical reactions and can generally be described by Maxwell's equations [5] and the continuity equation of charge which states that local electric charge density ρ changes by the divergence of the vector of current density $\vec{\imath}$:

$$\vec{\nabla} \cdot \vec{\imath} = -\frac{\partial \rho}{\partial t} . \quad (1)$$

If magnetic fields are neglected, the electrical field $\vec{E}$ is defined by the negative gradient of electric voltage V:

$$\vec{E} = -\vec{\nabla} V . \quad (2)$$

With the specific electric conductance σ, the electric displacement field $\vec{D}$ and the external vector of current density $\vec{\imath}_e$ the vector of current density $\vec{\imath}$ results to:

$$\vec{\imath} = \sigma \vec{E} + \frac{\partial \vec{D}}{\partial t} + \vec{\imath}_e . \quad (3)$$

In case of electrochemical machining the external current density equals zero because only an external voltage is applying. The electric displacement field is defined as:

$$\vec{D} = \varepsilon_0 \varepsilon_r \vec{E} . \quad (4)$$

Herein ε_0 is the electrical field constant and ε_r the material dependent relative permittivity. Altogether current density can be written as:

$$\vec{\imath} = \left(\sigma + \varepsilon_0 \varepsilon_r \frac{\partial}{\partial t}\right) \vec{E} . \quad (5)$$

2.2. Electrolyte

Flow fields of Newtonian fluids can completely be described by the Navier-Stokes equations [6]. Equivalent to the continuity equation of charge the conservation of mass can be written as:

$$\frac{\partial \rho}{\partial t} + \vec{\nabla} \cdot (\rho \vec{v}) = 0 . \quad (6)$$

Here ρ denotes fluid's density and $\vec{v}$ the velocity vector. If Newton's axioms are applied to a continuum the conservation of momentum results to:

$$\frac{\partial}{\partial t}(\rho \vec{v}) + \vec{\nabla} \cdot (\rho \vec{v}\vec{v}) = \rho \vec{g} - \vec{\nabla} p + \vec{\nabla} \cdot \bar{\bar{\tau}} . \quad (7)$$

Within equation (7) $\vec{g}$ is an acceleration vector, p the pressure and $\bar{\bar{\tau}}$ the tensor of shear stresses.

In ECM caused by the electrolysis of water hydrogen gas is produced on the cathode's surface. Therefore the fluid had to be described as a two phase flow which in general can be solved by the Navier-Stokes equations as well.

Caused by high flow velocities and sharp inlet angles of the cathodes, flow fields in ECM processes for aero engine components are mostly turbulent. In order to achieve adequate simulation times the Navier-Stokes equations are not computed directly. Hence turbulence has to be modeled separately e. g. by the k-ϵ-model [7].

2.3. Electrode Surface Reaction

To model the ECM process the mathematical description of surface reactions is of central importance. Basically current density i can be written as the difference of anode (index A) and cathode (index C) reactions:

$$i = i_A - i_C = Fk_A[Red] - Fk_C[Ox] . \quad (8)$$

Herein F is Faraday's constant and k represent the reaction velocities. These reaction velocities can be described with the help of the transition state theory and are defined as [8]:

$$k = Be^{-\frac{\Delta G}{RT}} . \quad (9)$$

According to Eyring's theory the temperature T dependent frequency factor B is proportional to the ratio of Boltzmann's (k_B) and Planck's (h) constant [9]:

$$B = \frac{k_B T}{h} . \quad (10)$$

Difference of free enthalpy (Gibbs free energy) ΔG is expressed by the sum of the enthalpy difference in the energetic ground state and the Galvani potential $\Delta\Phi$.

$$\Delta G = \Delta G(0) + F\Delta\Phi . \quad (11)$$

Equation (11) here denotes the maximum potential difference which does not occur in reality so that a passage factor α with $0 \leq \alpha \leq 1$ is applied.

If the anodic current density equals the cathodic current density, potential difference $\Delta\Phi$ equals the equilibrium rest potential E. This interrelationship leads to the exchange current density i_0:

$$i_A = i_{A0} e^{(1-\alpha)\frac{F}{RT}E} = i_0 , \quad (12)$$

$$i_C = i_{C0} e^{-\alpha\frac{F}{RT}E} = i_0 . \quad (13)$$

If an external potential E' is applied to the electrochemical cell, the potential within the cell changes from equilibrium rest potential to E' and the over-voltage η results on electrode's surfaces:

$$\eta = E' - E . \quad (14)$$

Hence the new potential difference $\Delta\Phi$ is:

$$\Delta\Phi = E + \eta . \quad (15)$$

Summarized and with the substitution $f = F/RT$ the local current density can be calculated by the so-called Butler-Volmer equation:

$$i = i_0\left(e^{(1-\alpha)f\eta} - e^{-\alpha f\eta}\right) . \quad (16)$$

2.4. Heat Transfer

In order to model an ECM-process the heat transfer is divided into heat transfer in solids and heat transfer in fluids under neglected thermal radiation. Based on the first law of thermodynamics and Fourier's law heat transfer in solids can be calculated by [6]:

$$\rho c_p \frac{\partial T}{\partial t} = \vec{\nabla}\cdot\left(k\vec{\nabla}T\right) + \sum_{i=0}^{n} q_i . \quad (17)$$

Herein c_p is the specific heat capacity, k the isotropic thermal conductivity and q_i a specific heat source.

In combination with the conservation of mass and momentum the conservation of energy for a fluid can be written as [6]:

$$\rho\frac{d}{dt}\left(e + \frac{\|\vec{v}\|^2}{2}\right) = \rho\vec{g}\cdot\vec{v} - \vec{\nabla}\cdot\left(k\vec{\nabla}T\right) - \vec{\nabla}\cdot(\rho\vec{v}) + \vec{\nabla}\cdot(\bar{\bar{\tau}}\cdot\vec{v}) + \sum_{i=0}^{n} q_i , \quad (18)$$

where e denotes the inner energy.

2.5. Ionic Transport Mechanisms

In general it is distinguished between the three types of ionic transport mechanisms diffusion, migration and convection [8].

Diffusion

Diffusion is described by Fick's laws. First Fick's law says that molecular particle flux J is proportional to the gradient of molar concentration c:

$$J = -D\frac{dc}{dx} . \quad (19)$$

Second Fick's law is a direct result of the first one and the conservation of mass for each element:

$$\frac{\partial c}{\partial t} = \vec{\nabla}\cdot\left(D\vec{\nabla}c\right) . \quad (20)$$

With the help of the Stokes-Einstein equation in which η is the dynamic viscosity of the fluid and R_0 ion's hydrodynamic radius, diffusion coefficient D can be calculated by:

$$D = \frac{k_B T}{6\pi\eta R_0} . \quad (21)$$

Migration

Ionic migration describes the movement of ions in an electric field. Positive charged ions move through the electric field in the direction of the negative pole. Assumed that the ions reach a stationary value of migration velocity, ionic mobility u can be calculated by the Nernst-Einstein equation. Therein R denotes the universal gas constant:

$$u = \frac{D}{RT} . \quad (22)$$

Convection

Finally dissolved particles can be moved by convection. This velocity is several orders of magnitude higher than diffusion or migration and can be described by the Navier-Stokes equations (cp. chapter 2.2). But the wall near boundary layer is an exception caused by the no-slip condition. In summary, all ionic transport mechanisms can be expressed for one species (index i) to equation (23). Therein R_i denotes a chemical reaction term:

$$\frac{\partial c_i}{\partial t} + \vec{\nabla}\cdot\left(-D_i\vec{\nabla}c_i - z_i u_i F c_i\vec{\nabla}V + c_i\vec{v}\right) = R_i \quad (23)$$

2.6. Faraday´s Law

Besides the complete description based on conservation equations the electrochemical machining process can approximately be described by Faraday's law [4]. For multiphase materials and due to the fact that

not each individual reaction is removal effective, Faraday's law can formally be written as:

$$V_{eff} = \frac{v_A}{i} = V_{sp}\eta = \frac{\eta}{\rho F}\sum_{i=1}\frac{w_i}{100}\frac{M_i}{\sum_{j=1} y_j z_{ij}} . \quad (24)$$

In equation (24) V_{eff} represents the effective material removal rate, v_A the dissolving velocity, V_{sp} the specific material removal rate, η the current efficiency, w_i the specific weight of the alloying addition i, M_i the molar mass and z_{ij} the electrochemical valence. Due to the fact that each element can be ionized differently strong, electrochemical valences in equation (24) are hard to forecast so that the adjustment factor y_j indicates the probability for each individual reaction taking place. But these probabilities are not known exactly because they are on their part a function of temperature, pH-value and so forth. For this reason and due to the fact, that the effective material removal rate can be determined very exactly in analogical experiments, values of V_{eff} are often used as basis for further simulations [10].

2.7. Physical Coupling

First of all the local current densities out of the Butler-Volmer equation (16) have to be coupled with Faraday's approach. Provided that all parameters for each elementary reaction i are known, the local, analytical dissolving velocities $v_{A,local}$ can be calculated by:

$$v_{A,local} = \sum_i \frac{M_i \upsilon_i i_i}{\varrho_i z_i F} . \quad (25)$$

Here υ_i denotes the stoichiometric coefficient of the reduced species i.

Up to now no general analytical expression for the conductance κ of strong electrolytes – as they are used in ECM – exists [11]. For this reason and due to the fact that this interrelationship is experimentally well proven, here a linear approach (slope factor β) is used to model κ as a function of temperature:

$$\kappa = \kappa_0 + \beta(T - T_0) . \quad (26)$$

Similar to equation (26) the electrical conductivity of two-phase flows can be calculated by semi-phenomenological approaches, e. g. of Bruggemann et al. [12].

Generally in ECM heat is generated by Joule heating and electrochemical reactions. Provided that nearly all electrical energy is converted into heat [13], Joule heating of the electrolyte q_{Joule} can be calculated in combination with Ohm's law to:

$$q_{Joule} = \Delta\varphi^2 \kappa s . \quad (27)$$

Therein $\Delta\varphi$ is the difference in potential between anode and cathode and s the local gap width. Due to their low specific resistances, Joule heating of used solids is neglected.

Heat generated by surface reactions can be expressed by the product of local current density i generated by Butler-Volmer reaction and over-voltage η:

$$q_{reaction} = i\eta . \quad (28)$$

Finally all equations of this chapter are introduced into one multi-physical model

3. Modeling and Simulation

3.1. Simulation Software

For modeling and simulation the commercial FE-software COMSOL Multiphysics has been used. Due to the modular design of this software tool it is possible to combine different physical phenomena together into one simulation model. COMSOL has already proven to be successful in several different electrochemical machining operations like jet-ECM [14] or in the manufacture of shaver caps [15].

3.2. Coupling Strategies

In order to solve the Butler-Volmer equation for each elementary reaction the exchange current density i_0 and the passage factor α has to be known. While α in most cases takes the value 0.5, values for i_0 unfortunately only exist for a small number of individual reactions [16]. Thus, currently it is not possible to set up a complete analytical model because many parameters are not existing and have to be found in future experimental studies.

Here Faraday's approach is used with the help of experimental data of the effective material removal rate V_{eff} [10]. In figure 2 simulation steps and possible coupling strategies are summarized by their names within COMSOL Multiphysics and particular physical effects they take into account.

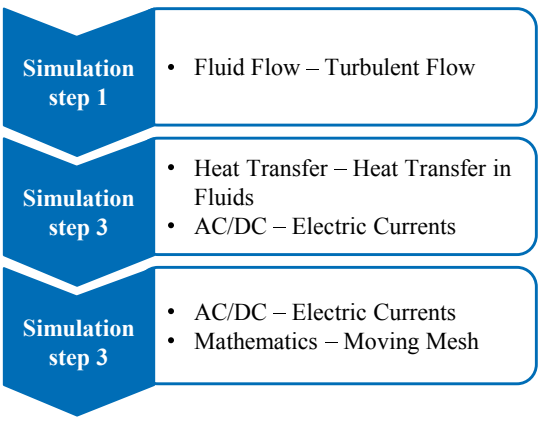

Fig. 2. Simulation steps and possible coupling strategies

3.3. Initial and Boundary Conditions

Table 1 summarizes typical initial and boundary conditions of ECM processes for the manufacture of aero engine components. Final simulation examples are based on these values. Aero engine components such as blades and blisks are manufactured in several steps so that feed rate and voltage are varied in a predefined range.

Table 1. Typical initial and boundary conditions

Initial and boundary condition	Symbol and physical unit	Value
Inflow temperature	T_i / K	308.15
Inflow conductivity of the electrolyte	κ_0 / (mS/cm)	55
Slope of the conductivity	β / (mS/(K·cm))	2.8
Feed rate	v_f / (mm/min)	0.3-1
Effective material removal rate	V_{eff} / (mm³/(A·s))	1.51
Voltage	U / V	7-20
Surrounding temperature	T_0 / K	298.15

4. Results and Discussion

In this chapter the results of simulation using the model with the initial and boundary conditions described above are presented for a real compressor blade application. Based on the blade target geometry itself and a cathode geometry which has proven to be successful in practice the simulation model is validated. In a second step a new inverted approach is presented where cathode geometry is computed.

4.1. Classic Simulation

Figure 4 shows schematically the ECM process of the manufacture of a compressor or turbine blade. Tool cathodes are moved with a constant feed rate towards the blade (anode) and due to local conditions of electrolysis the blade is formed.

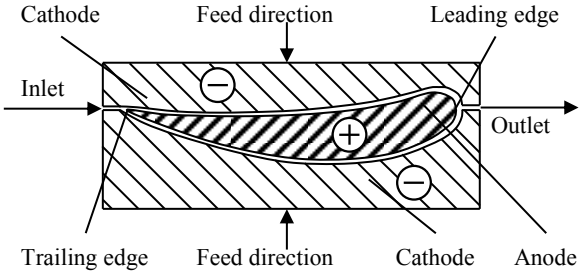

Fig. 3. Principle of ECM blade manufacture

Based on a real compressor blade geometry finally a simulation with the three simulation steps and couplings described above was made. Besides the target geometry a cathode geometry which has proven itself in practice was given in order to validate the simulation model. Figure 4 shows the results of the simulation. It is recognizable that the flow surfaces (detail 'c') are mapped excellent by the simulation in comparison to target geometry.

Geometrical deviations of less than 150 µm in trailing and leading edge can primarily be explained by inaccuracies of the predetermined inflow conductivity of the electrolyte. Another reason which is recognizable especially in detail 'a' is the low accuracy of splines generated by COMSOL. So a sharp trailing edge is built which does not correspond with the target geometry in this area.

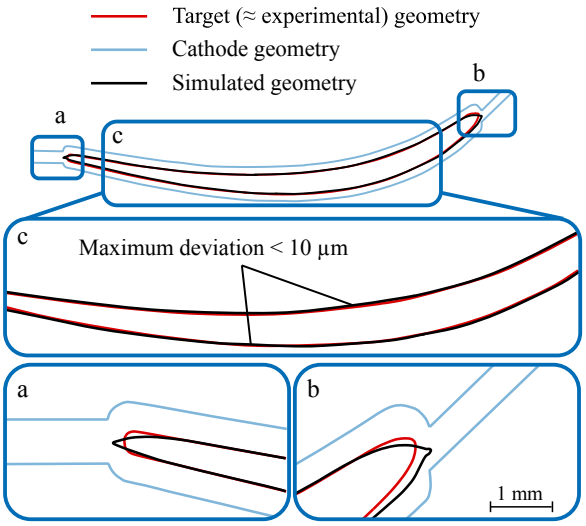

Fig. 4. Classic ECM process simulation

4.2. Alternative Cathode Calculation

Due to the fact that even with the help of a working simulation model the cathode design process would still be iterative now a new approach is presented. By inverting the electric field it is virtually possible to compute cathode geometry by using the target blade geometry as anode. ECM process is inverted so that later tool geometry forms itself due to local conditions of electrolysis and blade target geometry.

Figure 5 shows the results of this inverted approach for cathode design by comparing calculated geometry (black line) with the one already proven itself in practice (blue line). For the flow surfaces and the trailing edge good results can be stated and concerning the leading edge only in the area of profile's pressure side shows a slight difference between target and calculated contour. Electrolyte's specific resistance κ is of essential

importance for a successful model of the electrochemical removal process. At the moment κ_0 is only imprecisely determined at the inflow boundary and has to be improved in order to reach higher simulation accuracy.

It is impossible that cathodes cut themselves like in detail ‘a’ but that does not matter here because the aim of this calculation is to prove how near the simulation can map reality. Furthermore the inverse problem cannot be solved unique so that several solutions are possible.

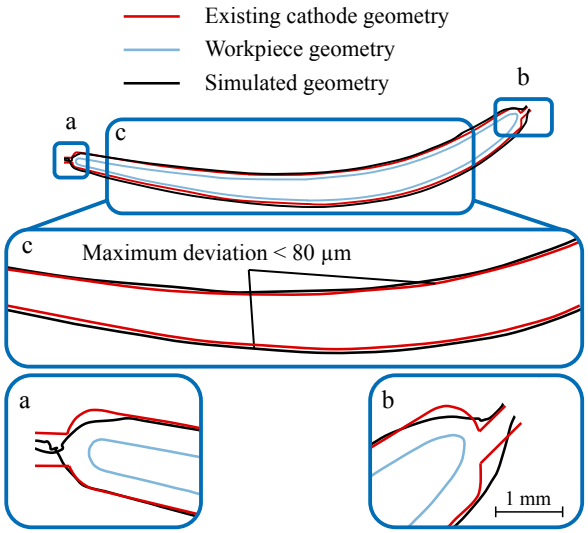

Fig. 5. Alternative cathode design simulation

5. Summary and Outlook

All necessary equations to describe the ECM process analytically and how they are connected to each other have been presented and discussed. With experimental results for the effective material removal rate according to Faraday’s law a simulation model has been built up taking into account fluid flow, electric field and heat transfer. In order to validate the simulation model a real compressor blade has been simulated in one aerodynamic cross-section in two different ways. Besides the simulation of the classical ECM process with the aim to calculate the blade contour by using predetermined cathode geometries a new inverted simulation strategy was presented. This new approach uses the blade target geometry in order to calculate the cathode shape by inverting the electric field. Both simulations showed good results compared to reality. To achieve even better results, the effects of the hydrogen evolution at the cathode have to be incorporated in the existing model. It is necessary to model the electrolyte either as a two-phase flow or to use a semi phenomenological approach which considers the gas phase influence to the conductivity of the electrolyte, e. g. of Bruggemann et al. In a next step a 3D-model is going to be built and by the here presented inverted approach a cathode is being calculated and manufactured. Afterwards a blade is going to be machined with this tool and measured as well as compared to target geometry.

Acknowledgements

This work has partially been funded by the German Federal Land NRW within the project EF 2037 ‘‘Vorschmieden und elektrochemische Fertigbearbeitung von Nickelbasis-Turbinenschaufeln für 700 Grad Dampfkraftwerke’’.

References

[1] Rajurkar K.P., Levy G., Malshe A., Sundaram M.M., McGeough A., Hu X., Resnick R., De Silva A., 2006, Micro and Nano Machining by Electro-Physical and Chemical Processes, CIRP Annals - Manufacturing Technology, 55:643–666.

[2] Klocke F., Zeis M., Klink A., Veselovac D., 2012, Technological and Economical Comparison of Roughing Strategies via Milling, EDM and ECM for Titanium- and Nickel-based Blisks, Proc. CIRP, 2:98-101.

[3] McGeough J.A., 1974, Principles of Electrochemical Machining, Chapman and Hall.

[4] Klocke F., Zeis M., Klink A., 2012, Technological and economical capabilities of manufacturing titanium- and nickel-based alloys via Electrochemical Machining (ECM), Key Engineering Materials, 504-506:1237-1242.

[5] Tipler P., Mosca G., 2004, Physik für Wissenschaftler und Ingenieure, Spektrum Akademischer Verlag.

[6] Schröder W., 2004, Fluidmechanik, Aachener Beiträge zur Strömungsmechanik, Wissenschaftsverlag Mainz in Aachen.

[7] Wilcox D., 1994, Turbulence Modeling for CFD, DCW Industries, Inc.

[8] Forker W., 1989, Elektrochemische Kinetik, Akad. Berlin Verlag.

[9] Steinfeld J., Francisco J., Hase W., 1998, Chemical Kinetics and Dynamics - Second Edition, Prentice Hall.

[10] Klocke F., Zeis M., Klink A., Veselovac D., 2013, Experimental Research on the Electrochemical Machining of Modern Titanium- and Nickel-based Alloys for Aero Engine Components, ISEM 2013, in press.

[11] Atkins P.W., de Paula J., 2006, Physikalische Chemie, Wiley-VCH.

[12] Kozak J., 1998, Mathematical models for computer simulation of electrochemical machining processes, Journal of Materials Processing Technology, 76/1-3:170-175.

[13] Kubeth H., 1965, Der Abbildungsvorgang zwischen Werkzeugelektrode und Werkstück beim Elektrochemischen Senken, Dissertation RWTH Aachen.

[14] Hackert M., 2009, Entwicklung und Simulation eines Verfahrens zum elektrochemischen Abtragen von Mikrogeometrien mit geschlossenem elektrolytischen Freistrahl, Dissertation TU Chmnitz.

[15] Van Tijum R., Pajak P.T., 2008, Simulation of Production Process using the Multiphysics approach: The Electrochemical machining Process, COMSOL Conference.

[16] Holze R., 2007, Electrochemistry, Springer.